M. BAKUMENKO,[1,2] V. BARDIK,[1] V. FARAFONOV,[3] D. NERUKH[2]

[1] Taras Shevchenko National University of Kyiv
(2, Prosp. Academician Glushkov, Kyiv 03022, Ukraine; e-mail: marynabakumenko@gmail.com, vital@univ.kiev.ua)
[2] Aston University
(Birmingham, B4 7ET, UK; e-mail: D.Nerukh@aston.ac.uk)
[3] V.N. Karazin Kharkiv National University
(4, Svobody Sq., Kharkiv 61022, Ukraine; e-mail: vsfarafonov@gmail.com)

THE MULTISCALE HYBRID METHOD WITH A LOCALIZED CONSTRAINT. II. HYBRID EQUATIONS OF MOTION BASED ON VARIATIONAL PRINCIPLES

UDC 539

A multiscale modelling framework that employs molecular dynamics and hydrodynamics principles has been developed to describe the dynamics of hybrid particles. Based on the principle of least action, the equations of motion for hybrid particles were derived and verified by using the Gauss principle of least constraints testifying to their accuracy and applicability under various system constraints. The proposed scheme has been implemented in a popular open-source molecular dynamics code GROMACS. The simulation for liquid argon under equilibrium conditions in the hydrodynamic limit ($s = 1$) has demonstrated that the standard deviation of the density exhibits a remarkable agreement with predictions from a pure hydrodynamics model, validating the robustness of the proposed framework.

K e y w o r d s: molecular dynamics, multiscale method, control volume function, hydrodynamic equations, equation of motion, Principle of least action, Gauss principle, constraint.

1. Introduction

A complex system of different scale levels offers a new overall knowledge of the physical characteristics of the entire system based on the fundamental level interactions of atoms and molecules. The significance of this description is approved and approaches, termed as multiscale methods, are currently developed quite actively [5, 13, 16–18, 20, 24, 25, 31]. The multiscale models have been successfully used in various fields of biological physics such as the dynamical properties of peptides [16], polymer dynamics [26, 27, 32, 33], structure, and a function of cell membranes [1, 15, 19, 21].

The key idea of the coupling between molecular dynamics (MD) and continuum mechanics is that atoms leave and enter the hydrodynamics part of the system. The fact that the atomistic and hydrodynamic components are separated by a border presents a significant conceptual challenge. The atomistic compo-

C i t a t i o n: Bakumenko M., Bardik V., Farafonov V., Nerukh D. The multiscale hybrid method with a localized constraint. II. Hybrid equations of motion based on variational principles. *Ukr. J. Phys.* **69**, No. 4, 269 (2024). https://doi.org/10.15407/ujpe69.4.269.

Ц и т у в а н н я: Бакуменко М., Бардик В., Фарафонов В., Нерух Д. Мультискейлінговий гібридний метод з локалізованим обмеженням. II. Гібридні рівняння руху, основані на варіаційних принципах. *Укр. фіз. журн.* **69**, №4, 269 (2024).

nent of the simulation is very sensitive to the location of the interface between the atomistic and hydrodynamic representations of the same fluid, so achieving the correct balance of mass and momentum flows across this boundary without introducing artefacts is a very important problem [13, 16, 17, 20, 24, 25].

In some approaches [9, 24, 25] the problem of the coupling between the atomistic and hydrodynamic phases is solved by establishing a finite-size overlapping zone, which gives a smoother transition between the particles and continuum parts of the system and provides the conservation of mass and momentum flows. The main disadvantage of these approaches is the introduction of the interpolation "switch" parameter, and it is generally unclear what this parameter means in the hybrid "buffer" region. A distinct method for state variable coupling which uses the modelling structure of a physical analogy to define the coupling terms in the "buffer" zone between the atomistic and hydrodynamic representations of the same liquid was presented in the works [20, 28].

Elaboration of the coupling approaches between MD and continuum for fluids dynamics compels a new class of constraints applied to the localized area Eulerian regions of space as opposed to the entire molecular domain. Thus, the important step in the development of the coupling approaches is inventing an appropriate technique to govern the microscale region in correlation with the continuum dynamics and the variational principles will therefore form the basis for these constraints. The equations of motion for accurately describing the connection between the MD and hydrodynamic representations are derived using the approach of constraints [24, 25]. These equations of motion serve as the foundation for numerous investigations in this area. The selection of constraint variables is a hotly debated topic, and, nowadays, there is no universal answer to the formation of a constraint procedure [3, 4, 6, 8].

The fundamental D'Alembert–Lagrange principle (DLP) has been applied to solve tasks with holonomic constraints and nonintegrable kinematic (nonholonomic) constraints [3, 8, 11]. DLP derives Lagrange's equations of state based on consideration of the instant state of the system and small virtual displacement to the particles position with constraints maintaining frozen during the displacement. However, the DLP application to general kinematic constraints with a general velocity and acceleration dependence has proven difficult, mostly due to the lack of a well-defined procedure that provides extracting the set of linear conditions that limit the virtual displacements from the constraint equations [6, 7].

Most of the literature data [4, 11, 24, 25, 31] illustrate that the variational Hamilton's principle is widely used for developing the constraint equations and for the further obtaining of equations of motion. As was shown [30], Hamilton's principle of least action provides deriving the correct equations of motion for the holonomic constraints, but the validity of its application remains obscure for nonholonomic and semi-holonomic constraints, while Gauss's principle is valid for these types of constraints [7]. The main goal of this work is to derive the hybrid equations of motion by the implementation of the variational Hamiltonian's Principle and the Gauss principle of least constraint. Following [31], we will apply the principle of least constraint to validate the principle of least action.

In our previous article [2], we proposed a new model of the hybrid particle for the multiscaling coupling using the control volume (CV) concept [14, 23, 29]. The system has been considered as a two-phase fluid: the Lagrangian and Eulerian representations correspond to the atomistic (MD) and the continuum (HD) phases, respectively. The proposed model is a reliable background for the future advance of the two-phase analogy model.

This article is the next stage in developing the hybrid two-phase multiscale model in the hydrodynamic limit within the framework of molecular dynamics software such as GROMACS.

2. Hamilton's Constrained Principle and Constraint Equations

The Hamilton's formulation of the principle of least action states that the dynamics of a physical system are determined by a variational problem for a functional based on the Lagrangian [11]

$$\delta A = \delta \int_{t_a}^{t_b} \mathcal{L}(\mathbf{q}_i, \dot{\mathbf{q}}_i) dt = 0. \tag{1}$$

Equation (1) represents the variation in the action (δA) over a given time interval from t_a to t_b, where $\mathcal{L}(q_i, \dot{q}_i)$ is the Lagrangian function depending on the generalized coordinates q_i and their time derivatives

$\dot{q}_i$. The condition $\delta A = 0$ corresponds to the principle of least action.

In Smith's work [31], the constraint equation sets the difference between the total momentum of a molecular CV and HD to be zero:

$$g(\mathbf{q}, \dot{\mathbf{q}}, t) = \sum_{n=1}^{N} m_n \dot{\mathbf{q}}_n \theta_n - \int\limits_V \rho \mathbf{U} dV = 0. \tag{2}$$

Based on the proposed definition of the hybrid mass developed using the modified CV function in [2], we build the constraint as the difference between the momentum of a hybrid particle in the hybrid zone and the total momentum of the MD and HD phases:

$$g_i = m_i \dot{\mathbf{q}}_i - \\ - \left((1-s) m_i' \, \dot{\mathbf{q}}_i' + s \sum_{k=1}^{N} \frac{1}{N_k} \mu_k(\mathbf{q}_i) \int \rho \mathbf{U} dV \right) = 0. \tag{3}$$

The introduced constraint is expressed, in general, by the equation

$$g_\alpha(\mathbf{q}, \dot{\mathbf{q}}, t) = 0 \tag{4}$$

and the type of this constraint is non-holonomic, as a function of position, velocity, and time [11].

The problem of the application of Hamilton's principle for the case of non-holonomic systems has been discussed by Flannery [6–8]. In this case, for a dynamical system without non-potential forces, Hamilton's constrained principle can be determined in the form

$$\delta A = \delta \int\limits_{t_a}^{t_b} \left(\mathcal{L}(\mathbf{q}_i, \dot{\mathbf{q}}_i) + \sum_{\alpha=1}^{C} \lambda_\alpha g_\alpha \right) dt = 0, \tag{5}$$

where C is the total number of constraints g_α and λ_α is a Lagrangian multiplier. Here, [4] constrained lagrangian $\mathcal{L}_\mathcal{C}$ is defined as:

$$\mathcal{L}_\mathcal{C} = \mathcal{L}(\mathbf{q}_i, \dot{\mathbf{q}}_i) + \sum_{\alpha=1}^{C} \lambda_\alpha g_\alpha. \tag{6}$$

The calculation of this variation produces the subsequent equation

$$\frac{d}{dt} \frac{\partial L}{\partial \dot{q}_i} - \frac{\partial L}{\partial q_i} = \sum_{\alpha=1}^{c} \left[\dot{\lambda}_\alpha \frac{\partial g_\alpha}{\partial \dot{q}_i} + \lambda_\alpha \left(\frac{d}{dt} \frac{\partial g_\alpha}{\partial \dot{q}_i} - \frac{\partial g_\alpha}{\partial q_i} \right) \right], \tag{7}$$

where it is assumed that the Lagrangian multiplier is a function of time. However, Flannery [7] showed that the following equation might be used to apply non-holonomic constraints (while Flannery demonstrated the possibility of applying non-holonomic constraints using the following equation):

$$\frac{d}{dt} \frac{\partial \mathcal{L}}{\partial \dot{\mathbf{q}}_i} - \frac{\partial \mathcal{L}}{\partial \mathbf{q}_i} = \sum_{\alpha=1}^{C} \lambda_\alpha \frac{\partial g_\alpha}{\partial \dot{\mathbf{q}}_i}. \tag{8}$$

Thus, the difference between Eq. (7) and Eq. (8) sets the condition for the so-called semi-holonomic constraints [30] in the form

$$\frac{d}{dt} \frac{\partial g_\alpha}{\partial \dot{\mathbf{q}}_i} - \frac{\partial g_\alpha}{\partial \mathbf{q}_i} = 0. \tag{9}$$

The substitution of constraint (3) into Eq. (9), and the statement that the time derivative of the mass of a hybrid particle is not zero (in contrast to Smith's approach [4]), demonstrates that the constraint of (3) is not semi-holonomic. The principle of least action should be verified by the Gauss Principle of least constraint, outlined in the next section. The Lagrange multiplier method is applied to obtain the equations of motion. The Euler–Lagrange equation is obtained by minimizing a constrained Lagrangian in Eq. (5)

$$\frac{d}{dt} \frac{\partial \mathcal{L}_C}{\partial \dot{\mathbf{q}}_i} - \frac{\partial \mathcal{L}_C}{\partial \mathbf{q}_i} = 0. \tag{10}$$

Using the definition of momentum based on a Lagrange function, one can obtain the conjugate momentum of particle i:

$$\mathbf{p_i} = \frac{\partial \mathcal{L}_C}{\dot{q}_i} = m_i (\dot{q}_i + \lambda_i). \tag{11}$$

The Lagrange multiplier can be defined by substituting Eq. (11) into constraint (3):

$$\lambda_i = \frac{\mathbf{p_i}}{m_i} - \frac{1}{m_i} \Bigg\{ (1-s) \, m_i' \, \dot{q}_i' + \\ + s \sum_{k=1}^{N} \frac{1}{N_k} \mu_k \left(q_i \right) \int \rho U dV \Bigg\}. \tag{12}$$

Thus, using expression (12) for λ in Eq. (11) yields the basic equations of motion for velocity in the form

$$\dot{\mathbf{q}}_i = \frac{1}{m_i} \left\{ (1-s) \, m_i' \, \dot{\mathbf{q}}_i' + s \sum_{k=1}^{N} \frac{1}{N_k} \mu_k(\mathbf{q}_i) \int \rho \mathbf{U} dV \right\}. \tag{13}$$

The substitution of Eq. (11) in Eq. (10) gives the time evolution of the momentum

$$\dot{p}_i = m_i\ddot{\mathbf{q}}_i + \dot{\mathbf{q}}_i\frac{dm_i}{dt} + \lambda_i\frac{dm_i}{dt} + m_i\dot{\lambda}_i, \tag{14}$$

where the time derivatives of mass

$$\frac{dm_i}{dt} = s\sum_{k=1}^{N}\frac{1}{N_k}\mu_k(\mathbf{q}_i)\frac{d}{dt}\int\rho dV + \\ + s\sum_{k=1}^{N}\frac{1}{N_k}\int\rho dV\frac{d\mu_k(\mathbf{q}_i)}{dt}, \tag{15}$$

the time derivative of the Lagrange multiplier

$$\dot{\boldsymbol{\lambda}}_i = \frac{1}{m_i}\left\{\dot{\mathbf{p}}_i - \frac{d}{dt}(1-s)\,m_i'\,\dot{\mathbf{q}}_i' - \right. \\ \left. - s\frac{d}{dt}\sum_{k=1}^{N}\frac{1}{N_k}\mu_k(\mathbf{q}_i)\int\rho\mathbf{U}dV\right\} + \\ + \frac{d}{dt}\left(\frac{1}{m_i}\right)\left\{\mathbf{p}_i - (1-s)\,m_i'\,\dot{\mathbf{q}}_i' - \right. \\ \left. - s\sum_{k=1}^{N}\frac{1}{N_k}\mu_k(\mathbf{q}_i)\int\rho\mathbf{U}dV\right\}. \tag{16}$$

Substituting Eq. (15) and Eq. (16) into Eq. (14), we have the equation in the form of Newton's law:

$$\ddot{\mathbf{r}}_i = \frac{1}{m_i}\mathbf{F}_i^{\mathrm{MD}} - \\ - \frac{1}{m_i}\left(s\sum_k\frac{1}{N_k}\mu_k\left(\dot{\mathbf{r}}_i\frac{d}{dt}\int\limits_V\rho dV - \frac{d}{dt}\int\limits_V\rho\mathbf{U}dV\right) + \right. \\ \left. + s\sum_k\frac{1}{N_k}C_k\dot{\mathbf{r}}_i\left(\dot{\mathbf{r}}_i\int\limits_V\rho dV - \int\limits_V\rho\mathbf{U}dV\right)\right), \tag{17}$$

where $\mathbf{F}_i^{\mathrm{MD}}$ represents the molecular dynamic force defined by the interaction between molecules, and the generalized coordinates $\mathbf{q}_i$ are replaced by the Cartesian coordinates $\mathbf{r}_i$. In the next section, Gauss's principle of least constraint will be applied for the validation of the obtained equation.

3. Gauss Principle of Least Constraint

The Gauss variational principle differs significantly from the DLP and Hamilton's principle. This principle provides a procedure of local minimization based on virtual displacements to the acceleration with the fixed state and yields the equations of state for both holonomic and nonholonomic systems [12, 22]

$$\frac{\partial}{\partial\ddot{r}_j}\left[\frac{1}{2}\sum_i^N m_i(r_i - \frac{F_i}{m_i})^2\right] = 0. \tag{18}$$

The advantage of Gauss's principle lies in its capability to incorporate nonholonomic constraints for a system with any number of degrees of freedom using Lagrangian multiplier $\boldsymbol{\lambda}_n$, expressed as:

$$\frac{\partial}{\partial\ddot{\mathbf{r}}_j}\left[\frac{1}{2}\sum_i^N m_i\left(\mathbf{r}_i - \frac{\mathbf{F}_i}{m_i}\right)^2 + \sum_i\lambda_i\dot{\mathbf{g}}_i\right] = 0. \tag{19}$$

This principle allows the consideration of constraints in systems with a variable number of degrees of freedom, making it particularly useful for a wide range of applications.

The uniqueness of our approach lies in the introduction of an individual constraint for each particle, as described in Eq. (3). By applying the Gauss principle, we differentiate Eq. (3) with respect to time and replace the generalized coordinates, $\mathbf{q}_i$, with the Cartesian coordinates, $\mathbf{r}_i$

$$\dot{\mathbf{g}}_i = m_i\ddot{\mathbf{r}}_i + s\sum_{k=1}^{N}\frac{1}{N_k}\frac{d\mu_k}{dt}\dot{\mathbf{r}}_i\int\rho dV + \\ + s\sum_{k=1}^{N}\frac{1}{N_k}\mu_k\dot{\mathbf{r}}_i\frac{d}{dt}\int\rho dV - \\ - \left((1-s)\mathbf{F}_i^{\mathrm{MD}} + s\sum_{k=1}^{N}\frac{1}{N_k}\frac{d\mu_k}{dt}\int\rho\mathbf{U}dV + \right. \\ \left. + s\sum_{k=1}^{N}\frac{1}{N_k}\mu_k\frac{d}{dt}\int\rho\mathbf{U}dV\right) = 0. \tag{20}$$

Then Eq. (19) can be simplified as

$$m_i\ddot{\mathbf{r}}_i - \mathbf{F}_i + \frac{\partial}{\partial\ddot{\mathbf{r}}_i}\left[\sum_n\eta_n\dot{g}_n\right] = 0 \tag{21}$$

and

$$m_i\ddot{\mathbf{r}}_i = \mathbf{F}_i - \eta_i m_i. \tag{22}$$

Substituting Eq. (22) into Eq. (20) gives the expression for Lagrange's multiplier

$$\lambda_i = \frac{1}{m_i}\left(s\sum_k\frac{1}{N_k}\frac{d\mu_k}{dt}\left[\dot{\mathbf{r}}_i\int\limits_V\rho dV - \int\limits_V\rho\mathbf{U}dV\right] + \right. \\ \left. + \mathbf{F}_i - (1-s)\mathbf{F}_i^{\mathrm{MD}} - s\sum_k\frac{1}{N_k}\mu_k\frac{d}{dt}\int\limits_V\rho\mathbf{U}dV\right). \tag{23}$$

Equation (23) substituted into (22) yields the expression for the hybrid acceleration in the form of Newton's second law

$$\ddot{\mathbf{r}}_i = \frac{1}{m_i}(1-s)\,\mathbf{F}_i^{\mathrm{MD}} - \\ - \frac{1}{m_i}\left(s\sum_k \frac{1}{N_k}\mu_k\left[\dot{\mathbf{r}}_i\frac{d}{dt}\int\limits_V \rho dV - \frac{d}{dt}\int\limits_V \rho\mathbf{U}dV\right] + \right. \\ \left. + s\sum_k \frac{1}{N_k}C_k\dot{\mathbf{r}}_i\left[\dot{\mathbf{r}}_i\int\limits_V \rho dV - \int\limits_V \rho\mathbf{U}dV\right]\right). \quad (24)$$

In the limiting case where $s = 0$, corresponding to the MD-phase, Eq. (24) reproduces Newton's second law

$$\ddot{\mathbf{r}}_i = \frac{1}{m_i}\mathbf{F}_i^{\mathrm{MD}}. \quad (25)$$

That implies the equivalence of the hybrid particle acceleration to the "pure" MD acceleration for a molecule in the absence of a hydrodynamic phase. The next extreme case, at $s = 1$, corresponds to the acceleration for the hydrodynamic phase

$$\ddot{\mathbf{r}}_i = \frac{1}{m_i}\left(\sum_k \frac{1}{N_k}\mu_k\left[\dot{\mathbf{r}}_i\frac{d}{dt}\int\limits_V \rho dV - \frac{d}{dt}\int\limits_V \rho\mathbf{U}dV\right] + \right. \\ \left. + \sum_k \frac{1}{N_k}C_k\dot{\mathbf{r}}_i\left[\dot{\mathbf{r}}_i\int\limits_V \rho dV - \int\limits_V \rho\mathbf{U}dV\right]\right). \quad (26)$$

The equation of motion (24) derived from the Gauss principle of least constraint is equivalent to Eq. (17), confirming the physical justification for applying the principle of least action in this case. These resulting equations demonstrate consistency and preserve their invariant form across extreme cases.

4. Simulation

The results of the simulation of liquid argon are presented in this part. The focus is on the calculation of the standard deviation (SD) of density fluctuations in the 3-D application as it is the quantity defining the thermal fluctuations in Landau–Lifshitz fluctuating hydrodynamics equations, the generalization of the Navier–Stokes equations for the scales below macroscopic, where the classical Navier–Stokes equations are valid.

Within this framework, the molecular density at the spatial point $\mathbf{r}_l$ can be computed by considering weighted contributions from the atoms within the CV, where the weights are determined by the CV itself. Here, the notation μ_l indicates that the CV is centered at $\mathbf{r}_l$, such that $\mu_l(\mathbf{r}_l) = 1$, and it linearly decreases to 0 at the boundaries of the CV

$$\rho_l^{md}(\mathbf{r}_l) = \sum_i \frac{m_i}{V}\mu_l(\mathbf{r}_i), \quad (27)$$

where the summation is performed over all atoms.

Then the time-averaged density variance at this point $\mathbf{r}_l$ is:

$$D\left(\rho_l^{md}(\mathbf{r}_l)\right) = \frac{1}{T}\sum_{t=1}^{T}\left(\left(\sum_i \frac{m_i}{V}\mu_l(\mathbf{r}_i)\right)_t^2 - \right. \\ \left. - \frac{1}{T^2}\left[\sum_{t=1}^{T}\left(\sum_i \frac{m_i}{V}\mu_l(\mathbf{r}_i)\right)_t\right]^2\right), \quad (28)$$

where T is the number of time steps over which averaging is carried out.

The hydrodynamics, density is discretely defined exclusively at the nodes comprising the simulation grid. The variance of hydrodynamic density at thOse nodes should be equal to the variance of molecular density. Specifically,

$$D\left(\rho_l^{md}(\mathbf{r}_l)\right) = D\left(\rho_k^{\mathrm{HD}}(\mathbf{r}_k)\right), \quad (29)$$

where $\mathbf{r}_k$ represents the position of the hydrodynamic (HD) node. This equality ensures that the hydrodynamic simulation accurately captures the variability in molecular density at the corresponding grid nodes.

From another perspective, the density at any given point can be estimated by employing a linear combination of densities from neighbouring nodes using the CV formulation. In this approach, the density at point $\mathbf{r}_l$, denoted as ρ_l, is considered as a linear combination of densities at nodes:

$$(\rho_l)^{\mathrm{lin}} = \sum_k \rho_k^{\mathrm{HD}}(\mathbf{r}_l)\,\mu_k(\mathbf{r}_l), \quad (30)$$

where the summation is performed over all nodes. Here, $\mu_k(\mathbf{r}_l)$ represents the weight assigned to each neighbouring hydrodynamics node.

Then the expression for the variance of a linear combination of densities can be expressed as

$$D\left((\rho_l)^{\mathrm{lin}}\right) = \frac{1}{T}\sum_{t=1}^{T}\left[\left(\sum_k \rho_k^{\mathrm{HD}}(\mathbf{r}_l)\mu_k(\mathbf{r}_l)\right)_t^2 - \right. \\ \left. - \frac{1}{T^2}\left(\sum_{t=1}^{T}\left(\sum_k \rho_k^{HD}(\mathbf{r}_l)\mu_k(\mathbf{r}_l)\right)_t\right)^2\right]. \quad (31)$$

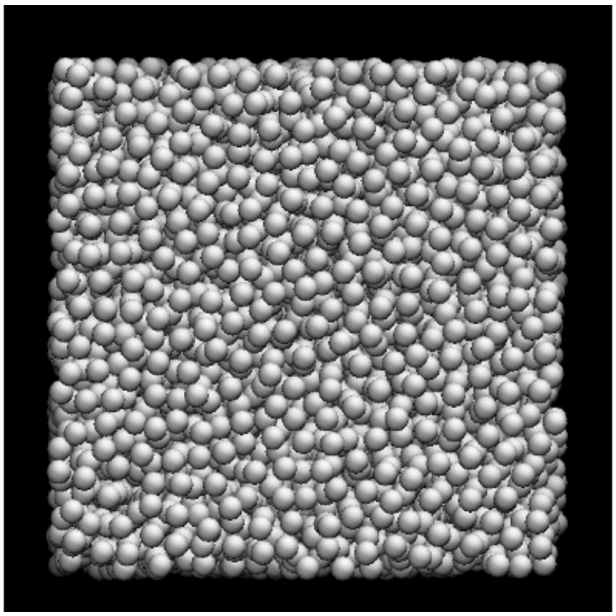

Fig. 1. A pre-equilibrated cell of liquid argon

According to the theorem on the variance of a linear combination [10], the variance of two random variables linearly combined is

$$\mathrm{Var}(aX+bY) = a^2\mathrm{Var}(X)+b^2\mathrm{Var}(Y)+2ab\mathrm{Cov}(X,Y). \tag{32}$$

In the assumption of non-correlated variables, their covariance is equal to zero, which makes the variance a linear combination of variances of each variable multiplied by the squares of the coefficients. In the Landau–Lifshitz fluctuating hydrodynamics framework the random fluctuations of the density values at different locations (nodes) are independent, therefore, their variance is

$$D\left((\rho_l)^{\mathrm{lin}}\right) = {\mu^2}_k(\mathbf{r}_l)\left[\frac{1}{T}\sum_{t=1}^{N}\left(\sum_i \frac{m_i}{V}\mu_k(\mathbf{r}_i)\right)_t^2 - \right.$$

$$\left. - \frac{1}{T^2}\left[\sum_{t=1}^{N}\left(\sum_i \frac{m_i}{V}\mu_k(\mathbf{r}_i)\right)_t\right]^2\right]. \tag{33}$$

Thus,

$$D\left(\rho_l\right)^{\mathrm{lin}} = \sum_k \mu_k^2\left(\mathbf{r}_l\right) D\left(\rho_l^{\mathrm{HD}}\right). \tag{34}$$

Therefore, the assessment of SD is accomplished by employing the suggested control volume formulation, expressed as:

$$\mathrm{SD}\left((\rho_{\mathbf{r}_l})^{\mathrm{lin}}\right) = SD(\rho^{\mathrm{HD}})\sqrt{\sum_k(\mu_k(\mathbf{r}_l))^2}. \tag{35}$$

Here, ρ_{r_l} signifies the hydrodynamic density at the point $\mathbf{r}_l$, $\mu_k(\mathbf{r}_l)$ denotes a control volume function centered at $\mathbf{r}_k$, and it serves as a representation of the weight assigned to hydrodynamic grid nodes. This formulation enables a refined assessment of the standard deviation of the density within the simulation grid, incorporating the influence of hydrodynamic factors and contributing to a more accurate depiction of density fluctuations in the hydrodynamic context.

Since the sum of all μ_k at any location is always 1, the sum of their squares is less than 1. Therefore, the linear interpolation of the hydrodynamic density underestimates the correct standard deviation of the density. The SD of the density should be equal to the SD of the random term in LL-FH equations, and it should also coincide with the SD of the density computed using atoms, as in equation (28).

At the next stage, the equations of motion were implemented in the GROMACS 2016.4 software suite. The Fluctuating Hydrodynamics (FH) subsystem was introduced using the previously developed Landau Lifshitz Fluctuating Hydrodynamics (LL-FH) solver [16, 17] The test system was a cubic cell filled with liquid argon (Fig. 1). It was initially equilibrated for 10 ns by means of standard molecular dynamics.

The parameters were as follows: temperature of 86.5 K, maintained by means of a Nose-Hoover thermostat, time step of 2 fs, and van der Waals interactions were switched off between 1.0 and 1.2 nm.

The productive hybrid simulation lasted for 1 ns under the same conditions, which was sufficient to obtain converged results. In this simulation, s was chosen to equal 1.0, indicating that atom motion followed only hydrodynamic fields with no contribution from interatomic dispersion-repulsion forces. Consequently, the thermostat was turned off.

The fluctuating hydrodynamics (FH) density and momentum fields were discretized over a $3\times3\times3$ grid and updated every 10 MD time steps. During each update, the density and momentum val-

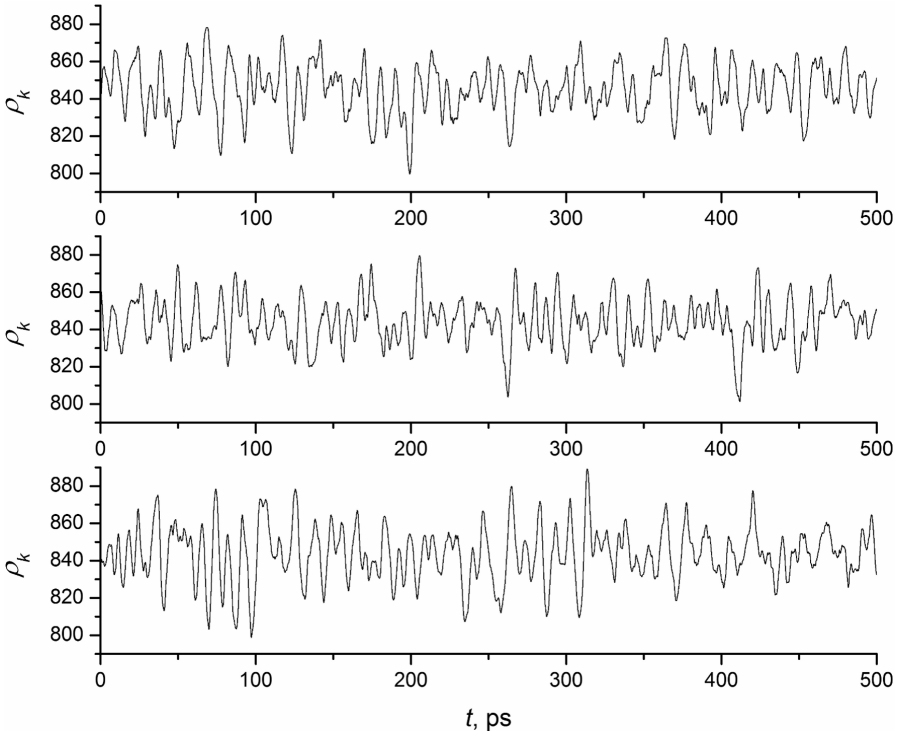

Fig. 2. Time course of FH density of three FH cells during the hybrid simulation

ues in the FH grid nodes were assigned random values obtained from a Gaussian distribution with a mean of 843.9 a.m.u./nm^3 or 0 nm/ps, respectively, and a standard deviation of 14.61 a.m.u./nm^3 or 0.0103 nm/ps, respectively. Each 100 MD steps, the $\Sigma\mu_k^2$ and ρ_i values of each atom were saved to a file for a further analysis. An example of the time course of FH density assigned to three FH grid nodes is shown in Fig. 2.

The data collected during the hybrid simulation were compared with the prediction of Eq. (31). The set of hybrid densities of atoms was binned with respect to $\sqrt{\sum \mu_k^2}$ into 0.05-wide bins. The predicted range for $\sqrt{\sum \mu_k^2}$ spans from 0.5 (when $\mu_1 = \mu_2 = \mu_3 = \mu_4 = 0.25$) to 1.0 (when any μ value equals 1.0, and the rest are 0.0), resulting in 10 bins.

The standard deviation of the hybrid density for each bin was calculated over atoms with $\sqrt{\sum \mu_k^2}$ falling into the corresponding range. The values of $\mathrm{SD}(\rho_i)$ are plotted in Fig. 3 versus the average $\sqrt{\sum \mu_k^2}$. The standard deviation of FH densities in the FH grid nodes randomly generated during the simulation equalled 13.91 a.m.u./nm^3. With this

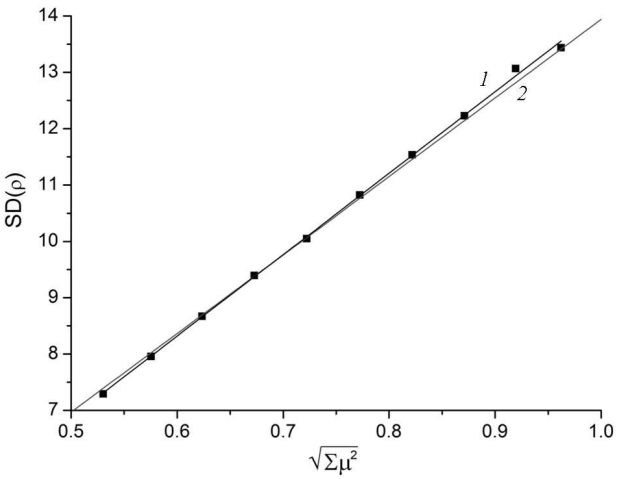

Fig. 3. The standard deviation of hybrid density between atoms having different $\sqrt{\sum \mu_k^2}$ values is depicted. Black points represent values from MD simulation-hybrid equations at $s = 1$, the black line indicates a linear fit, and the red line represents the prediction from Eq. (31)

value, Eq. (31) shows a good correspondence with the $\mathrm{SD}(\rho_i)$ computed over densities of hybrid particles located between the grid nodes.

5. Conclusions

The principle of least action has been applied to the previously developed multiscale model based on the modified control volume function [2]. The equations of motion for hybrid particles are derived. The validity of the obtained equations is confirmed by the application of the Gauss principle.

The simulation has demonstrated, in the hydrodynamic limit, the standard deviation of the density in the hybrid system of matches. The predictions of pure hydrodynamics are obtained, which testifies to the validity of the proposed model in describing the hybrid system dynamics.

The next objective is to extend the simulation procedure to explore a range of the hybridization parameters that will give a more comprehensive understanding of the system's behavior. Thus, the proposed multiscale approach will provide valuable insights into the complex interplay between molecular dynamics and hydrodynamics of hybrid systems and, therefore, can be viewed as a starting point for the development of more complicaed models, e.g., for biomolecules or more complex liquids.

We thank the European Union's Horizon 2020 research and innovation program under the Marie Sklodowska-Curie Research and Innovation Staff Exchange, MSCA-RISE-2018, Proposal number: 823922, AMR-TB for financial support. V.F. and D.N. acknowledge the use of the HPC Midlands supercomputer funded by EPSRC, grant number EP/P020232/1; the access to HPC Call Spring 2021, EPSRC Tier-2 Cirrus Service; the access to the Sulis Tier 2 HPC platform hosted by the Scientific Computing Research Technology Platform at the University of Warwick. Sulis is funded by EPSRC grant EP/T022108/1 and the HPC Midlands + consortium. This study was partially supported by the Simons Foundation (USA) via grant number 1030292.

1. G. Ayton, G.A. Voth. Bridging microscopic and mesoscopic simulations of lipid bilayers. *Biophys. J.* **83**, 3357 (2002).
2. M. Bakumenko, V. Bardik, D. Nerukh. The multiscale hybrid method with a localized constraint. I. A modified control volume function for the hybridized mass and momentum equations. *Ukr. J. Phys.* **68**, 8 (2023).
3. A.M. Bloch. *Nonholonomic Mechanics and Control* (Springer, 2003).
4. E. Smith. *On the Coupling of Molecular Dynamics to Continuum Computational Fluid Dynamics* (Imperial College London, 2013).
5. G. De Fabritiis, R. Delgado-Buscalioni, P.V. Coveney. Multiscale modeling of liquids with molecular specificity. *Phys. Rev. Lett.* **97** (13), 134501 (2006).
6. M.R. Flannery. The elusive d'Alembert–Lagrange dynamics of nonholo-nomic systems. *American J. Phys.* **79**, 932 (2011).
7. M.R. Flannery. D'Alembert–Lagrange analytical dynamics for nonholo-nomic systems. *J. Math. Phys.* **52** (3), 032705 (2011).
8. M.R. Flannery. The enigma of nonholonomic constraints. *Am. J. Phys.* **73** (3), 265 (2005).
9. E.G. Flekkoy, G. Wagner, J. Feder. Hybrid model for combined particle and continuum dynamics. *Europhysics Lett.* **52**, 271 (2000).
10. D. Freedman, R. Pisani, R. Purves. *Statistics* (W.W. Norton & Company, 2007).
11. H. Goldstein, C. Poole, J. Safko. Classical mechanics. *American J. Phys.* **70** (7), 782 (2002).
12. D.T. Greenwood. *Advanced Dynamics* (Cambridge University Press, 2003).
13. J. Hu, I.A. Korotkin, S.A. Karabasov. A multi-resolution particle/fluctuating hydrodynamics model for hybrid simulations of liquids based on the two-phase flow analogy. *J. Chem. Phys.* **149** (8), 084108 (2018).
14. J.H. Irving, J.G. Kirkwood. The statistical mechanical theory of transport processes. IV. The equations of hydrodynamics. *J. Chem. Phys.* **18** (6), 817 (1950).
15. P.M. Kasson, V.S. Pande. Cross-graining: Efficient multiscale simu-lation via Markov state models. *Pacific Symposium on Biocomputing* **15**, 260 (2010).
16. I. Korotkin, S. Karabasov, D. Nerukh *et al.* A hybrid molecular dynamics/fluctuating hydrodynamics method for modelling liquids at multiple scales in space and time. *J. Chem. Phys.* **143** (1), 014110 (2015).
17. I.A. Korotkin, S.A. Karabasov. A generalised Landau–Lifshitz fluctuating hydrodynamics model for concurrent simulations of liquids at atomistic and continuum resolution. *J. Chem. Phys.* **149** (24), 244101 (2018).
18. E. Kotsalis, J. Walther, E. Kaxiras, P. Koumoutsakos. Control algorithm for multiscale flow simulations of water. *Phys. Revi. E* **79** (4), 045701(R) (2009).
19. R. Lonsdale *et al.* A multiscale approach to modelling drug metabolism by membrane-bound cytochrome P450 enzymes. *PLoS Computational Biology* **10**, e1003714 (2014).
20. A. Markesteijn, S. Karabasov, A. Scukins *et al.* Concurrent multiscale modelling of atomistic and hydrodynamic processes in liquids. *Philos. Trans. R. Soc. A* **372** (2021), 20130379 (2014).
21. J. Marrink *et al.* The MARTINI force field: Coarse grained model for biomolecular simulations. *J. Phys. Chem. B* **111** (27), 7812 (2007).
22. G.P. Morriss, C.P. Dettman. Thermostats: Analysis and application. *Chaos* **8** (2), 321 (1998).
23. N. Nangia, H. Johansen, N. Patanka *et al.* A moving control volume approach to computing hydro- dynamic forces

and torques on immersed bodies. *J. Computational Phys.* **347**, 437 (2017).
24. X.B. Nie, S.Y. Chen, W.N. E, M.O. Robbins. A continuum and molecular dynamics hybrid method for micro-and nano-fluid flow. *J. Fluid Mech.* **500**, 55 (2004).
25. S.T. O'Connell, P.A. Thompson. Molecular dynamics–continuum hybrid computations: A tool for studying complex fluid flows. *Phys. Rev. E* **52** (6), R5792 (1995).
26. J.T. Padding, W.J. Briels. Systematic coarse-graining of the dynamics of entangled polymer melts: The road from chemistry to rheology. *J. Phys.: Condensed Matter* **23**, 233101 (2011).
27. J.T. Padding, W.J. Briels. Time and length scales of polymer melts studied by coarse-grained molecular dynamics simulations. *J. Chem. Phys.* **117**, 925 (2002).
28. E. Pavlov, M. Taiji, A. Scukins *et al.* Visualising and controlling the flow in biomolecular systems at and between multiple scales: from atoms to hydrodynamics at different locations in time and space. *Faraday Discussions* **169**, 285 (2014).
29. C.S. Peskin. The immersed boundary method. *Acta Numerica* **11**, 479 (2002).
30. E.J. Saletan, A.H. Cromer. A variational principle for nonholonomic systems. *American J. Phys.* **38** (7), 892 (1970).
31. E.R. Smith, D.M. Heyes, D. Dini, T.A. Zak. A localized momentum constraint for non-equilibrium molecular dynamics simulations. *J. Chem. Phys.* **142** (7), 074110 (2015).
32. N.A. Spenley. Scaling laws for polymers in dissipative particle dynamics. *Europhys. Lett.* **49**, 534 (2000).
33. V. Symeonidis, G. Em Karniadakis, B. Caswell. Dissipative particle dynamics simulations of polymer chains: Scaling laws and shearing response compared to DNA experiments. *Phys. Rev. Lett.* **95**, 076001 (2005).

Received 21.02.24

М. Бакуменко, В. Бардик, В. Фарафонов, Д. Нерух

МУЛЬТИСКЕЙЛІНГОВИЙ ГІБРИДНИЙ МЕТОД З ЛОКАЛІЗОВАНИМ ОБМЕЖЕННЯМ. II. ГІБРИДНІ РІВНЯННЯ РУХУ, ОСНОВАНІ НА ВАРІАЦІЙНИХ ПРИНЦИПАХ

ля опису динаміки гібридних частинок було розроблено систему мультискейлінгового моделювання, що використовує принципи молекулярної динаміки та гідродинаміки. Ґрунтуючись на принципі найменшої дії, ми отримали рівняння руху гібридних частинок, які узгоджуються із принципом найменших обмежень Ґауса, що свідчить про їхню точність та застосовність при різних обмеженнях, накладених на систему. Запропоновану схему використано при моделюванні рівноважного стану рідинного аргону в рамках пакету GROMACS. Продемонстровано узгодженість отриманих стандартних відхилень густини з результатами суто гідродинамічного моделювання, що підтверджує надійність запропонованої моделі.

Ключові слова: молекулярна динаміка, мультискейлінговий метод, функція контрольного об'єму, гідродинамічні рівняння, рівняння руху, принцип найменшої дії, принцип Ґауса, обмеження.